International Journal of Chemical Engineering and Applications, Vol. 2, No. 1, February 2011
ISSN: 2010-0221

Pyrolytic Carbons from Porogen-treated Rice Husk as Lithium-insertion Anode Materials

G.T.K. Fey[1*], Y.D. Cho[1], C.L. Chen[1], K.P. Huang[1], Y.C. Lin[1], T.P. Kumar[1], and S.H. Chan[2]

***Abstract*—Structural and lithium insertion characteristics of high-capacity disordered carbons derived from rice husk are described. The carbonaceous materials were synthesized by pyrolyzing rice husk under argon with and without prior treatment with a proprietary porogenic agent. Both the porogen-free and porogen-treated precursors yielded carbons with poor crystallinity, although the surface areas of the latter products were six to nine-fold higher. The small values of the R factor, as determined from XRD data, suggested that all the carbons were predominantly non-parallel single sheets of carbons. The high capacities of these disordered carbons are attributed to lithium that bound to the hydrogen-saturated carbons and also onto extra surfaces of the single layers of carbon. Other contributing factors are the accommodation of additional lithium in the nanoscopic cavities, interaction of lithium with surface functional groups, and lithium plating on the carbon surface. Although disadvantaged by high first-cycle irreversible capacities, the carbons derived from porogen-treated precursors delivered high capacities at increasing coulombic efficiencies as the cycling proceeded. The consistently high capacities make them potential candidates as anode materials for lithium-ion batteries.**

***Index Terms*—carbonaceous anode, high-capacity carbons, lithium-ion batteries, rice husk.**

I. Introduction

Carbonaceous materials manifest themselves in a variety of crystallographic and morphological forms. Apart from the hundreds of industrial varieties, several carbonaceous materials have been synthesized in the laboratory, often by the pyrolysis of organic precursors. Although all forms of carbons can insert lithium, the extent of lithium intake and the reversibility of the reaction are determined by their lattice arrangement, surface texture, surface functional groups, etc. [1, 2]. Pyrolytically derived carbons have a disordered structure and often contain substantial amounts of hydrogen. These carbons have demonstrated lithium insertion capacities much larger than the 372 mAh/g theoretically possible with perfectly graphitic structures [3-5]. However, the high irreversible capacities of these carbons [6, 7] even after several cycles [8] and the large hysteresis in the charge-discharge profiles of hydrogen-containing carbons [7, 9] continue to be major disadvantages. Despite these shortcomings, disordered carbons are pursued for their potential applicability in practical devices.

[1]Dept. of Chemical and Materials Engineering, National Central University, Chung-Li, Taiwan 32054 R.O.C. (*Author for correspondence: Tel/Fax: +886-3-425-7325; E-mail: gfey@cc.ncu.edu.tw)
[2]Fuel Cell Center, Yuan Ze University, Chung-Li 32003, Taiwan, R.O.C.

In addition to their advantages of high lithium intake capacities and good cyclability, disordered carbons can be structurally modified by varying the nature of their organic precursors and temperature protocols. Disordered carbons obtained by pyrolysis of organic precursors contain a predominantly planar hexagonal network of carbons, but lack extended crystallographic ordering. Pyrolytic carbons have also been known to retain up to 30 at. % of residual hydrogen [3]. The high lithium capacities in pyrolytically prepared carbon varieties have been found to be associated with both disorder [10, 11] and hydrogen content [11, 12]. Although several models have been proposed to account for the additional capacity exhibited by disordered carbons [2, 13, 14], it is hard to satisfactorily account for the simultaneous large capacities and the voltage hysteresis in highly porous carbons with H/C ratios of less than 0.05 [15]. The absence of long-range order frustrates attempts at understanding the structure–reversible lithium intercalation properties of these carbons.

Among the cheapest and most abundant precursors for disordered carbons are biomass materials like sugar [16], cotton wool [17], coconut shells [18], rice husk [19, 20], sugarcane bagasse [21], starch and oak [22], walnut and almond shells [22], and peanut kernels [12]. Fey et al. [12] reported that peanut kernel-derived carbons delivered first-cycle insertion capacities as high as 4765 mAh/g, the highest lithium intake capacities reported so far. It is also noteworthy that disordered carbons derived from rice husk maintained good reversibility upon repeated cycling, the first and fifth-cycle deinsertion capacities being 1055 and 1051 mAh/g, respectively [19]. In our previous study, we have investigated the pyrolytic carbons obtained from rice treated with different concentrations of HCl or NaOH [23]. In this paper, we report the results of our study on the structural, morphological and electrochemical features of pyrolytic carbons from porogen-treated rice husk.

II. Experimental

Carbon samples for this work were synthesized as described elsewhere [19]. Cleaned and dried rice husk was stirred for 24 h with an aqueous solution of a proprietary porogenic agent and dried. The amount of porogen used was such that the weight ratios of the rice husk to the porogen were 1:1, 1:2, 1:3, 1:4 and 1:5 (hereinafter referred to as P = 1, 2, 3, 4 and 5, respectively). The porogen-treated rice husk samples were then heated at 150 ºC for 1 h, followed by a 1-h calcination at 500, 600, 700, 800 and 900 ºC. The calcined samples were refluxed in HCl, washed till the pH of the

washing was 7, dried, and ground into fine powders.

Elemental analysis was carried out on a Perkin Elmer CHN 2400 elemental analyzer. Powder x-ray diffractometry was performed (Siemens D 5000 MacScience MXP 18 x-ray diffractometer) with nickel-filtered Cu K radiation. The data were collected between scattering angles (2θ) of 5º and 80º in steps of 0.05º. A Sieko SSC 5000 TG/DTA equipment was used for thermal analysis. The analysis was done in argon between room temperature and 900 ºC at a heating ramp of 10 ºC /min with a 50 mg sample. BET surface area measurements were carried out on a Micromeritics ASAP 2010 surface area analyzer. The surface morphology of the carbons was examined by scanning electron microscopy (Hitachi S-4700I). Laser Raman spectroscopic measurements were performed in the 1200-1700 cm-1 region with a laser radiation wavelength of 632.8 nm (Renishaw G-17868 Raman spectrophotometer). The Raman results were fitted with Renishaw software.

Coin cells of the 2032 configuration were assembled as described earlier [19]. Galvanostatic charge-discharge profiles were recorded between 3.00 and 0.005 V at a 0.1C rate on a Maccor Series 4000 multi-channel battery tester. The carbons studied are designated in this paper as C-n-x, where n stands for the porogen/rice husk weight ratio, and x for the temperature at which the rice husk was pyrolyzed.

III. Results and Discussion

A. Thermal analysis

The TG and DTA curves recorded with the porogen-free and porogen-treated (P = 5) rice husk samples between room temperature and 900 ºC are shown in Fig. 1 and Fig. 2. The endotherm and the corresponding weight loss centered around 100 ºC in Fig. 1 are due to the loss of superficial moisture and other light volatiles from the husk. In their studies on the thermal degradation of rice husk in nitrogen, Mansaray and Ghaly [24] found that the active pyrolysis zone for rice husk was in the 184–380 ºC range. This zone is attributed to the evolution of volatiles emanating upon decomposition of primary hemicellulose and cellulose [24]. Between about 400 and 500 ºC, a major change in the slope of the TG curve can be seen. This region, known as the passive pyrolysis zone, indicates a second reaction zone, and is attributed to lignin conversion [24]. Further weight loss up to about 800 ºC suggests that some reaction involving the char was continuing.

The differential thermogram shown in the inset has two weight loss regions, around 330 and 390 ºC in the active pyrolysis zone. It has been reported [24] that hemicellulose decomposes mainly between 150 and 350 ºC, cellulose between 275 and 350 ºC, and lignin decomposes gradually between 250 and 500 ºC. Thus, the first degradation step in the active pyrolysis zone involves the decomposition of hemicellulose and the initial decomposition stages of cellulose, while the second degradation step would involve the final stages of cellulose decomposition and the initial stages of lignin decomposition [24]. It must be noted that the temperature ranges for the decomposition reactions depend on the variety of rice husk as well as on the heating rate [24].

The TG and DTA patterns of the porogen-treated rice husk (P = 5) are shown in Fig. 2. It can be seen that the porogen decomposes in the active pyrolysis zone of rice husk, which is a critical factor in aiding the formation of pores. The extra heat generated by the decomposition of the porogen aids the sluggish formation and subsequent organization of the carbon layers. As in the porogen-free sample, the passive pyrolysis region is associated with further loss of volatile vapors and aromatic condensation processes that are part of the intricate pyrolytic reactions.

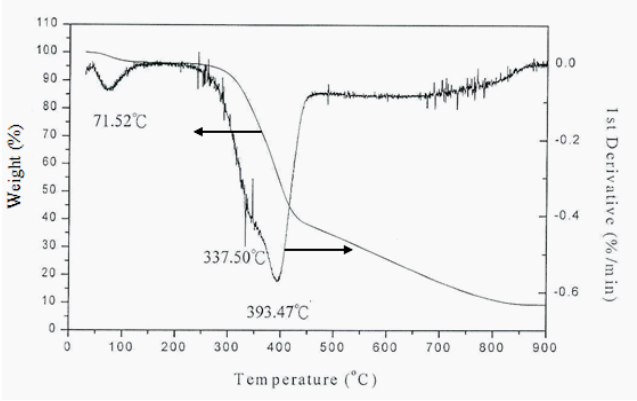

Fig. 1. Thermal behavior of porogen-free in argon.

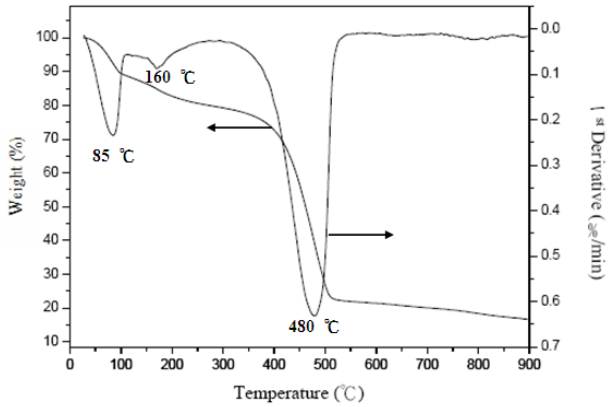

Fig. 2. Thermal behavior of porogen-treated (P = 5) rice husk in argon

B. X-ray diffraction

Powder x-ray diffractograms of the products obtained by pyrolysis of the porogen-free rice husk at different temperatures are presented in Fig. 3. The XRD patterns represent those of highly disordered carbons. The evolution of the characteristic (002) peak with increasing temperature can be seen. The broad (002) reflections between 20° and 30° indicate small domains of coherent and parallel stacking of the graphene sheets. In other words, graphite-like domains began to evolve as the temperature increased. Even the lowest value of d200 values (3.770Å for the C-0-500 sample) was substantially higher than the d002 value for graphite (3.345Å). In an earlier paper [19], we ascribed this increase in d002 value to interstitial silicon in the inter-layer spacings. However, it must be noted that since d002 values are the averages of a multitude of layer spacings, they can be somewhat misleading because in turbostratically disordered carbon structures the spacings between non-parallel layer pairs can be much larger than the spacings between parallel layer pairs.

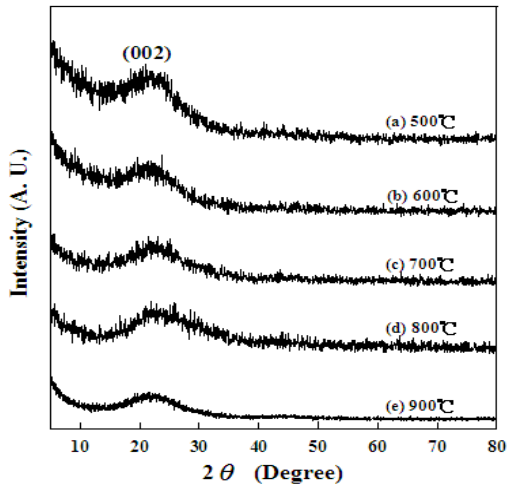

Fig. 3. Powder x-ray diffractograms of the products obtained by pyrolysis of the porogen-free rice husk at different temperatures.

Fig. 4 presents the powder x-ray diffraction patterns of carbons derived from porogen-treated rice husk (P = 5) at different temperatures. Again, a distinctive evolution of the (002) reflection can be noted with increasing temperature. The increased ordering of the aromatic layers at high temperatures is reflected in the diffractograms. Even after accounting for the fact that any extra heat evolved during the decomposition of the porogen favored an alignment of the unorganized layers in the carbons, the observation that d002 spacings diminished with increasing temperature for these carbons is contrary to the trend with carbons from porogen-free precursors.

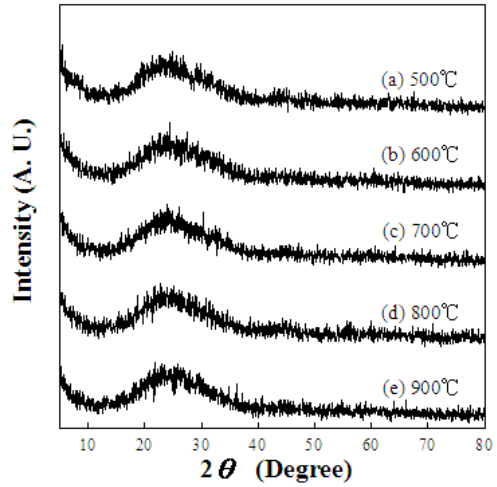

Fig. 4. Powder x-ray diffractograms of the products obtained by pyrolysis of the porogen-treated (P = 5) rice husk at different temperatures.

The ratio of the height of the (002) Bragg reflection to the height of the background, defined by the empirical parameter, R, is a measure of the fraction of single layered carbon sheets in disordered carbons. Such layers can provide lithium accommodation sites on both sides. Because these single layers are not arranged in parallel, a large number of pores or voids also form between them. Accordingly, materials with the largest single layer fraction will have the highest capacity for lithium insertion.

The R parameters were calculated from the x-ray data for the carbon samples (Table I). They were the lowest for the carbons prepared at 500 ℃ from porogen-free precursors, which indicates that these materials were made up of a large number of unorganized single graphene layers. However, the R factor values of the porogen-free husk-derived carbons increased as the pyrolysis temperature was raised. At the higher temperatures, there was more thermal energy to mobilize the individual graphene layers into parallel layers. Thus, as more single carbon layers align themselves into small domains of ordered structures, the carbon tends to be increasingly graphitic in nature. These structural characteristics have direct implications on the electrochemical performance of the carbon as lithium-insertion anodes. A similar trend in the R parameter was observed in the case of the carbons derived from the porogen-treated precursors, although the corresponding values were larger than those for the porogen-free precursor-derived carbons (1.67 for the C-0-500 sample). Thus, porogen has a definitive effect on the alignment of the graphene layers. Finally, an increase in the R parameter with the porogen content was also observed, supporting the above supposition. Porogens are not normally expected to alter the crystallographic parameters of the products. However, the diminished d002 spacings and the higher R values for the carbons derived from the porogen-treated rice husk must be attributed to additional heat energy provided by the decomposition of the porogen or by the subsequent reaction of porogen with the carbonaceous matrix.

TABLE I . ELEMENTAL ANALYSIS DATA, AVERAGE INTER-LAYER SPACINGS AND R FACTOR VALUES OF THE DIFFERENT CARBONACEOUS PRODUCTS.

Sample name	Percentage composition				Average Interlayer distance (Å)	*R*-factor
	C	H	N	H/C		
C-1-500	68.94	2.58	1.65	0.45	3.857	1.92
C-2-500	71.09	2.32	2.24	0.39	3.822	2.51
C-3-500	70.16	2.43	2.41	0.42	3.754	2.00
C-4-500	67.79	2.18	1.90	0.39	3.753	2.24
C-5-500	67.48	2.07	1.96	0.37	3.713	2.10
C-5-600	73.35	1.76	0.72	0.29	3.720	2.10
C-5-700	67.51	1.55	0.58	0.28	3.751	2.60
C-5-800	66.37	1.38	0.57	0.25	3.696	2.64
C-5-900	66.05	1.16	0.55	0.21	3.695	2.68

C. Raman spectroscopy

Raman spectroscopy is a useful tool for the study of carbons because Raman spectral response is sensitive to the microscopic structure of the carbon. Raman spectra of the C-1-500, C-3-500 and C-5-500 carbons are shown in Fig. 5. Two bands can be seen in all the spectra: one, the D-band around 1355 cm-1, and the other, the G-band around 1580 cm-1. The G-band is an inherent Raman-active band for the ideal graphite structure, corresponding to the E2g vibration mode [25], and ascribed to the C—C stretching in the longitudinal symmetry axis of the graphite plane [26]. The D-band, usually identified as the A1g mode, is forbidden for the two-dimensional lattice of graphite according to selection rules, and is a subject of controversy [27]. However, for graphite crystallites of finite sizes, the A1g mode will become Raman-active. This band is assigned to defects on the boundary of the carbon layers. The G-band also became sharper, indicating a high degree of graphitization in the products.

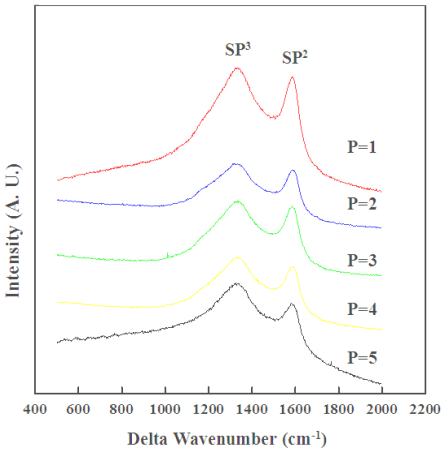

Fig. 5. Raman spectra of the carbons obtained from rice husk precursors containing different porogen contents.

Table II shows the positions of the characteristic Raman bands and the integrated intensity ratios (ID/IG) of the carbon samples treated at 500 ℃. Although the C-1-500 sample gave the highest individual peak intensities and seemingly contravened our assumption on the effect of porogen, the highest intensity ratio value was registered by the C-5-500 sample. The integrated intensity ratio is a measure of the orientation of the graphitic planes and the degree of graphitization [28].

TABLE II. POSITIONS OF THE CHARACTERISTIC RAMAN PEAKS AND THEIR INTEGRATED INTENSITY RATIOS

P	Peak (cm^{-1})		Integrated Area (A)	A_{SP3}/A_{SP2}
1	SP^3	1319.9	5812000	7.20
	SP^2	1584.6	807430	
2	SP^3	1311.9	2955700	7.45
	SP^2	1586.6	396600	
3	SP^3	1321.1	3218700	7.48
	SP^2	1580.5	430440	
4	SP^3	1317.1	3329400	7.71
	SP^2	1586.1	431910	
5	SP^3	1308.6	6580100	14.74
	SP^2	1588.1	446290	

D. Galvanostatic charge-discharge studies

We have already shown [19] that C-0-500 was not electro-active, and that among the carbons derived from porogen-free precursors, the highest first-cycle insertion capacity was obtained with C-0-700, whose capacity was 691 mAh/g. The inactivity of C-0-500 is due to (i) the temperature being too low for sufficient carbonization-aromatization of the products, and (ii) the insignificant number of micropores, which are not retained once they are formed by the evolving gases. However, in carbons derived at temperatures above the carbonization temperature, the micropores formed can be retained. Any coalescence of the small pores to yield large ones may only serve to increase surface area, and disfavor their function as cavities in which lithium can be stored.

In contrast, the carbons derived from the porogen-treated rice husk were shown to be highly electro-active even when the pyrolysis temperature was maintained at 500 ºC. In fact, as shown in Table III, the first-cycle insertion capacities for C-1-500, C-2-500, C-3-500, C-4-500 and C-5-500 were 1190, 2226, 2259, 3253 and 2374 mAh/g, respectively. The corresponding irreversible capacities were 62, 61, 62, 69 and 56 %. Thus, the P = 5 sample was found to yield the highest deinsertion capacity and the cycle efficiency. Therefore, a decision was made to study the effect of pyrolysis temperature on the capacity of carbons derived from the P = 5 precursors. As the pyrolysis temperature was raised to 600 ºC, the first-cycle insertion capacity rose to 2523 mAh/g (C-5-600, see Table IV). However, a further increase in temperature reduced the first-cycle insertion capacity: 2507, 1598 and 1530 mAh/g, respectively, for C-5-700, C-5-800 and C-5-900. The fact that the porogen-laden rice husks yielded carbons with higher capacities indicates that the decomposition of the porogen provided sufficient energy for the carbonization-graphitization processes. It is most obvious in the case of the carbons obtained at 500 ºC. While the C-0-500 material gave a paltry 7 mAh/g, the C-5-500 material could insert a remarkable 2374 mAh/g equivalent of lithium.

TABLE III. LITHIUM INSERTION CAPACITIES OF CARBONS DERIVED FROM RICE HUSK TREATED WITH DIFFERENT AMOUNTS OF POROGEN. PYROLYSIS TEMPERATURE: 500 ºC. CHARGE-DISCHARGE: 0.1 C RATE; 3.000~0.005V.

C.N.	P = 1				P = 2				P = 3				P = 4				P = 5			
	I.C.	D.C.	Ir.C.	C.E.	I.C.	D.C.	Ir.C.	C.E.	I.C.	D.C.	Ir.C.	C.E.	I.C.	D.C.	Ir.C.	C.E.	I.C.	D.C.	Ir.C.	C.E.
1	1190	457	733	38	2226	868	1358	39	2259	853	1406	38	3253	1023	2230	31	2374	1055	1319	44
2	654	508	146	78	931	875	56	94	1028	839	189	82	1040	867	173	83	1107	1063	44	96
3	590	516	74	87	868	850	18	98	942	835	107	89	842	808	34	96	1129	987	142	87
4	590	529	61	90	896	839	57	94	903	814	89	90	746	714	32	96	1161	1035	126	89
5	608	554	54	91	849	792	57	93	858	793	65	92	762	714	48	94	1128	1051	77	93

TABLE IV. EFFECT OF TEMPERATURE ON THE CHARGE-DISCHARGE BEHAVIOR OF P = 5 CARBONS. CHARGE-DISCHARGE: 0.1 C RATE; 3.000~0.005V.

C.N.	500 ℃				600 ℃				700 ℃				800 ℃				900 ℃			
	I.C.	D.C.	Ir.C.	C.E.	I.C.	D.C.	Ir.C.	C.E.	I.C.	D.C.	Ir.C.	C.E.	I.C.	D.C.	Ir.C.	C.E.	I.C.	D.C.	Ir.C.	C.E.
1	2374	1055	1319	44	2523	1448	1075	57	2507	923	1584	37	1598	604	994	38	1530	536	994	35
2	1107	1063	44	96	1546	1178	368	76	1125	915	210	81	749	642	7	86	768	607	161	79
3	1129	987	142	87	1330	1162	168	87	1033	935	98	91	788	732	56	93	764	661	103	87
4	1161	1035	126	89	1268	1157	111	91	935	832	103	89	773	722	51	93	769	691	78	90
5	1128	1051	77	93	1243	1144	99	92	895	810	84	91	716	699	17	98	779	719	60	92

The high first-cycle insertion capacities and the attendant irreversible capacities are attributed to the high H/C ratios of these low-temperature pyrolytic carbons [3, 6], as well as to the presence of a large number of nanopores [29]. According to Dahn et al. [3, 6] hydrogen-containing carbons show capacities proportional to their hydrogen content and exhibit large hysteresis. They suggest that such low-temperature carbons have an abundance of nanopores. It can be seen from Table I that the H/C ratio is 0.37 for the C-5-500 sample. This ratio decreased gradually as the temperature was raised. The low resolution of the characteristic (002) reflections coupled with the small value of the R factor (2.10) suggest that these low-temperature carbons had a predominance of randomly stacked single layers of carbon that can provide double surfaces for lithium accommodation as well as nanopores that can lodge more lithium. The low R factors suggest that under their formation conditions, there was insufficient thermal energy for graphene layers to rotate into a parallel alignment in accordance with Dahn's 'falling cards model' [30]. Thus, the low-temperature carbons have a large number of non-parallel, unorganized single layers of carbon. The presence of such uncorrelated graphene fragments plays an important role in the amount of lithium that a carbon sample can insert [3]. As the formation temperature of the carbons is increased, the thermal energies reach values high enough to break the links between adjacent sheets and favor their alignment into parallel orientations. As a result, not only are more and larger domains of organized regions formed (increasing the value of the R factor), but larger pores are also formed. In accordance with this model, carbon samples prepared at higher temperatures should have fewer unorganized single layers of carbon and nanopores, which should account for the lower lithium storage capacities.

For some of the carbons the deinsertion capacities were found to increase with cycling. It can also be seen that although the first-cycle irreversible capacity generally became lower with increasing pyrolysis temperature, a greater percentage was lost with increasing temperature. Interestingly, the coulombic efficiencies for the charge-discharge processes improved with cycling. Mention must be made of the high reversible capacities of the carbons, particularly of C-5-500. They were consistently much higher than the 372 mAh/g, the maximum theoretical capacity that can be tapped from perfectly graphitic structures. Thus, it appears that although the first-cycle irreversible capacities of the carbons were high, they were unique in that they continued to deliver high capacities. This is illustrated in Fig. 6, which presents the long-cycling behavior of C-5-700 at 0.1 and 0.2 C rates. Capacity was remarkably constant even beyond 150 cycles. Thus, if the first-cycle irreversible capacity loss in these carbonaceous materials can be suppressed, the porogen-treated rice husk carbons would be attractive anode materials for lithium-ion batteries.

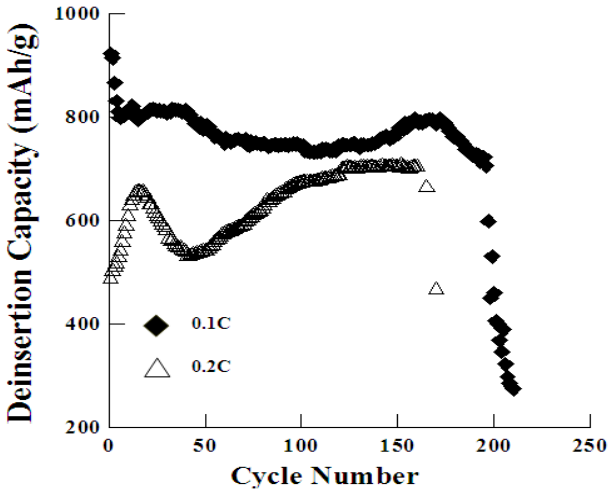

Fig. 6. Cycling behavior of C-5-700 carbon at 0.1 and 0.2 charge-discharge rates. Voltage range: 3.000~0.005V.

IV. Conclusions

Prolytic carbons derived from porogen-treated rice husk have been shown to possess high lithium insertion capacities. The high capacities in these disordered carbons are believed to be due to the binding of lithium to the hydrogen-saturated carbons and onto the extra surfaces of the single layers of carbon. Although the first-cycle irreversible capacities of the carbons were high, they continued to deliver high capacities at increasing coulombic efficiencies as the cycling proceeded. The remarkably constant and high capacities make them potential candidates as anode materials for lithium-ion batteries.

References

[1] S. Flandrois, A. Fevrier-Bouvier, K. Guerin, B. Simon, and P. Biensan, "On the electrochemical intercalation of lithium into graphitizable carbons," Mol. Cryst. Liq. Cryst., vol. 310, 1998, pp. 389-396.
[2] I. Cameán, P. Lavela, José L. Tirado, and A.B. García, "On the electrochemical performance of anthracite-based graphite materials as anodes in lithium-ion batteries," Fuel, vol. 89, 2010, pp. 986-991.
[3] J.R. Dahn, T. Zheng, Y.H. Liu, and J.S. Xue, "Mechanisms for lithium insertion in carbonaceous materials," Science, vol. 270, 1995, pp. 590-598.
[4] G.T.K. Fey, D.C. Lee, and Y.Y. Lin, "High-capacity carbons prepared from acrylonitrile-butadiene-styrene terpolymer for use as an anode material in lithium-ion batteries," J. Power Sources, vol. 119–121, 2003, pp. 39-44.
[5] A. Manuel Stephan, T. Prem Kumar, R. Ramesh, S. Thomas, S.K. Jeong, and K.S. Nahm, "Pyrolitic carbon from biomass precursors as anode materials for lithium batteries," Mater. Sci. Eng. A, vol. 430, 2006, pp. 132-137.
[6] T. Zheng, J.S. Xue, and J.R. Dahn, "Lithium insertion in hydrogen-containing carbonaceous materials," Chem. Mater., vol. 8, 1996, pp. 389-393.
[7] Y.J. Hwang, S.K. Jeong, J.S. Shin, K.S. Nahm, and A. Manuel Stephan, "High capacity disordered carbons obtained from coconut shells as anode materials for lithium batteries," J. Alloys Comp., vol. 448, 2008, pp. 141-147.
[8] M. Alamgir, Q. Zuo, and K.M. Abraham, "Behavior of carbon electrodes derived from poly(p-phenylene) in polyacrylonitrile-based polymer electrolyte cells," J. Electrochem. Soc., vol. 141, 1994, pp. L143-L144.
[9] H. Fujimoto, A. Mabuchi, K. Tokumitsu, and T. Kasuh, "Irreversible capacity of lithium secondary battery using meso-carbon micro beads as anode material ," J. Power Sources, vol. 54, 1995, pp. 440-443.
[10] Y. Liu, J.S. Xue, T. Zheng, and J.R. Dahn, "Mechanism of lithium insertion in hard carbons prepared by pyrolysis of epoxy resins," Carbon, vol.33, 1996, pp. 193-200.
[11] D.Y. Park, D.Y. Park, Y.Lan, Y.S. Lim, M.S. Kim, "High rate capability of carbonaceous composites as anode electrodes for

lithium-ion secondary battery," J. Ind. Eng. Chem., vol. 15, 2009, pp. 588-594.
[12] G.T.K. Fey, D. C. Lee, Y.Y. Lin, and T. Prem Kumar, "High-capacity disordered carbons derived from peanut shells as lithium-intercalating anode materials," Synth. Met., vol. 139, 2003, pp. 71-80.
[13] H. Fujimoto, K. Tokumitsu, A. Mabuchi, and T. Kasuh, "New structural parameters for carbon: comprehensive crystallization index and cavity index," Carbon, vol. 32, 1994, pp. 1249-1252.
[14] J. C. Arrebola,A. Caballero, L. Hernán, J. Morales, M. Olivares-Marín, and V. Gómez-Serranob, "Improving the Performance of Biomass-Derived Carbons in Li-Ion Batteries by Controlling the Lithium Insertion Process," J. Electrochem. Soc., vol. 157, 2010, pp. A791-A797.
[15] J. Gong and H. Wu, "Electrochemical intercalation of lithium species into disordered carbon prepared by the heat-treatment of poly (p-phenylene) at 650 °C for anode in lithium-ion battery," Electrochim. Acta, vol. 45, 2000, pp. 1753-1762.
[16] G.T.K. Fey, K.L. Chen, and Y.C. Chang, "Effects of surface modification on the electrochemical performance of pyrolyzed sugar carbons as anode materials for lithium-ion batteries," Mater. Chem. Phys., vol. 76, 2002, pp. 1-6.
[17] E. Peled, V. Eshkenazi, and Y. Rosenberg, "Study of Lithium Insertion in Hard Carbon Made from Cotton Wool," J. Power Sources, vol. 76, 1998, pp. 153-158.
[18] Y.J. Hwang, S.K. Jeong, J.S. Shin, K. S. Nahm, and A. Manue Stephan, "High capacity disordered carbons obtained from coconut shells as anode materials for lithium batteries," J. Alloys Comp., vol. 448, 2008, pp. 141-147.
[19] G.T.K. Fey and C.L. Chen, "High-capacity carbons for lithium-ion batteries prepared from rice husk," J. Power Sources, vol. 97-98, 2001, pp. 47-51.
[20] T.H. Liou, "Evolution of chemistry and morphology during the carbonization and combustion of rice husk," Carbon, vol. 42, 2004, pp. 785-794.
[21] E.Y. Matsubara, S.M. Lala, and J.M. Rosolen, "Lithium Storage into Carbonaceous Materials Obtained from Sugarcane Bagasse ," J. Braz. Chem. Soc., vol. 21, 2010, pp. 1877-1884.
[22] W. Xing, J.S. Xue, T. Zheng, A. Gibaud, and J.R. Dahn "Correlation between lithium intercalation capacity and microstructure in hard carbons," J. Electrochem. Soc., vol. 143, 1996, pp. 3482-3491.
[23] G.T.K. Fey, Y.D. Cho, C.L. Chen, Y.Y. Lin, T. Prem Kumar, and S.H. Chan, "Pyrolytic carbons from acud/base-treated rice husk as lithium-insertion anode materials," vol. 82, 2010, pp.2157-2165.
[24] K.G. Mansaray and A.E. Ghaly, "Thermal degradation of rice husks in nitrogen atmosphere," Bioresource Technol., vol. 65, 1998, pp. 13-20.
[25] F. Tunistra and J.L. Koenig, "Raman spectrum of graphite," J. Phys. Chem., vol. 53, 1970, pp. 1126-1130.
[26] A.C. Ferrari and J. Robertson, "Interpretation of raman spectra of disordered and amorphous carbon," Phys. Rev. B, vol. 61, 2000, pp. 14095-14107.
[27] R. Escribano, J.J. Sloan, N. Siddique, N. Sze, and T. Dudev, "Raman spectroscopy of carbon-containing particles," Vibr. Spec., vol. 26, 2001, pp. 179-186.
[28] H. Groult, B. Kaplan, S. Komaba, N. Kumagai, V. Gupta, T. Nakajima, and B. Simon, "Lithium Insertion into Carbonaceous Anode Materials Prepared by Electrolysis of Molten Li-K-Na Carbonates," J. Electrochem. Soc., vol. 150, 2003, pp. G67-G75.
[29] K. Tokumitsu, A. Mabuchi, H. Fujimoto, and T. Kasuh, "Charge/discharge characteristics of synthetic carbon anode for lithium secondary battery," J. Power Sources, vol. 54, 1995, pp. 444-447.
[30] J.R. Dahn, W. Xing, and Y. Gao, "The falling cards model for the structure of microporous carbons," Carbon, vol. 35, 1997, pp.825-830.